Astron. Astrophys. 362, L9–L12 (2000)

ASTRONOMY AND ASTROPHYSICS

LETTER

Letter to the Editor

The contribution of Oxygen to the "30", "26" and "20" μm features

R. Papoular

Sce Chimie Moleculaire, CEA Saclay, 91191 Gif-s-Yvette, France
(papoular@scm.saclay.cea.fr)

Received 4 September 2000 / Accepted 13 September 2000

Abstract. The IR absorption spectra of several macromolecules of interest for amorphous carbonaceous cosmic dust were simulated by means of a commercially available state-of-the-art chemical code. None of the three unidentified far IR features show up significantly in the absence of oxygen in the structure. By contrast, peripheral OH (hydroxy) gives rise to strong modes in the "30" band. The "26" and "20" bands are brought forth by O-bridges and O-substituted 5-membered carbon rings and enhanced by the OH's. A few similar macromolecules containing various small amounts of oxygen in these three forms and combined in various proportions are enough to qualitatively fit typical dust spectra recently extracted from ISO observations.

Key words: molecular processes – radiation mechanisms: thermal – ISM: dust, extinction – ISM: planetary nebulae: general – infrared: ISM: lines and bands

1. Introduction

The unidentified "30" μm feature is a very broad feature which extends from about 22 to about 45 μm. It was discovered by Forrest et al. (1981) and further studied by Szcerba et al. (1999). More recently, Hrivnak et al. (2000; HVK, for short, in the following) succeeded in extracting remarkably good spectra of this feature from the ISO observations of several stars (see also Volk et al. 2000). As a consequence, they were able to resolve it into a broad "30" μm feature and a narrower feature at 25.5 μm (to be designated by "26" in the following). The unidentified "21" μm feature (to be designated below by "20") was discovered by Kwok et al. (1989) and further studied by Volk et al. (1999) and Omont et al. (1995). It peaks around 20-21 μm and has a FWHH of about 2μm.

All 3 features are seen in emission and only towards extreme carbon stars (continuous circumstellar shell) and PPNe (protoplanetary nebulae; detached circumstellar shell), i.e. at stellar evolutionary stages between the end of the AGB and the PN. As a consequence of the fast transit through these stages and of the location of the features in the FIR, the catalog of such stars is still sparse. It appears, however, that these features are mostly seen together with different relative intensities and I suggest here that they are all due, partly at least, to oxygen atoms, in different bonding forms, in the mostly carbonaceous carrier of the UIBs (Unidentified InfraRed Bands). This, of course, is not exclusive of other contributions, such as TiC for the 20-μm band (von Helden et al. 2000).

The model of carbonaceous carrier used in this work was elaborated over the years (Papoular et al. 1996; Papoular 2000) to fit the UIBs, which are now generally assigned to the atomic vibrations of different groups of mainly C and H atoms. In the present model, these groups form an amorphous structure including oxygen, which also contributes to the 6.2, 7.7 and 8.6 μm features, as well as other heteroatoms: sulfur and nitrogen. The composition and structure of such materials are known to evolve under heat and radiation processing in the ISM (Inter-Stellar Medium; see Papoular (1996)). It is shown here that, in these materials, oxygen atoms in the form of hydroxy groups (OH), as bridges between aromatic clusters and in pentagonal carbon are, respectively, the main contributors to the "30", "26" and "20" features. Because of the evolving and highly inhomogeneous composition and structure of the carrier material, the strengths of the 3 bands relative to each other and to the mid-ir UIBs may vary considerably in space and time, as observed in the sky. It will appear that amorphous, inhomogeneous, grains made mainly of C, H and O, with C in both aromatic and aliphatic structures, can display all the bands considered here.

2. The chemical software

The spectrum observed in the sky is radiated by the overall, time-dependent,electric dipole moment resulting from the vibrations of atoms in the carrier. The spectral distribution and intensities of these vibrations depend on the way the carrier is excited and, especially, on the average energy content of the carrier, due to this excitation (Papoular 2000). It will be assumed, here, that the carrier is in thermal equilibrium with the ambient radiation field, which is also supposed to be characteristic of a warm black body (100 to 200 K). Under such circumstances, the emission spectrum scales as the product of Planck's law and the absorption spectrum of the material. This is the spectrum

Send offprint requests to: R. Papoular

Table 1. Macromolecular dust components

No	Name	N_{at}	O_{tot}	OH	O_{penta}	O_{bridge}	S	N	I(30)	I(26)	I(20)	Use	Nb(fit)
1	R(ref)	101	8	5	1	2	2	1	146	19	38	all	4
2	R-heter	105	0	0	0	0	0	0	14	7	2		–
3	R-OH	95	3	0	1	2	1	1	14	9	40	20	3
4	Arom 1	106	4	0	0	4	0	0	10	20	7	26	17
5	Aliph 1	50	6	6	0	0	0	0	88	5	0	30	3
6	Arom 2	110	8	4	0	4	0	0	163	23	12	30;26	1
7	Aliph 2	75	8	6	0	2	0	0	253	15	19	30;20	1
8	R-N (1)	101	7	4	1	2	2	0	160	19	29	all	2
9	R-N (2)	93	9	6	1	2	1	0	258	25	18	all	3
10	R-N-OH	97	3	0	1	2	2	0	14	8	14	UIB	–

of the 3N-6 discrete, harmonic vibrations (normal modes) into which one can break down any motion of the N atoms constituting the carrier particle. When the energy of this motion is low and non-linear effects due to anharmonicity can be neglected, the spectrum can be calculated directly from the force field between the atoms. This was carried out as follows, using the Hyperchem package released by Hypercube, Inc. in 1999, and implemented on a desk-top PC equipped with a Pentium (r) II processor (480 MHz) and MMX (TM) technology.

First, the model carrier is built on the screen by picking atom after atom in a table of elements. The CC bondings are specified graphically:-,=,≡, - - - . A computational code and options are then selected. Here, I used the semi- empirical PM3 code (see Stewart 1989).

Using its internal library of force fields corresponding to the selected structure, the code then optimizes the molecular geometry, i.e. determines the architecture which minimizes the total potential energy. This positions all the atoms at the bottom of their potential wells in any vibrational mode. The computation of the spectrum then reduces to simple matrix operations. For each normal mode, it yields a frequency and an IR intensity, I (km/mole), a quantity proportional to the particle absorbance α at that particular frequency.

Even when life-time broadening is taken into account, such spectra are discrete, and they are sparser the smaller the carrier. By contrast, the most highly resolved celestial spectra display relatively broad features. In the present dust model, this is due first and foremost to inhomogeneous broadening: each normal mode frequency is characteristic of the whole particle composition and structure, since all the atoms are more or less involved in each mode; because we are not dealing with small, free-flying, molecules, even carriers of the same family are likely to differ slightly in composition and/or structure, so their characteristic frequencies will all be shifted relative to each other; given enough variety (disorder) in a single particle and/or enough different particles along the line of sight, "continuous" *bands* will form by blending of crowded *lines*.

With the computational gear used here, it is hard to manage more than about one hundred atoms per particle, and the calculated spectra remain discrete ($\leq$ 0.1 mode/cm^{-1} on average). However, since so "small" a particle cannot carry all the diversity required to emulate the obseved spectra, it was necessary to merge the spectra of several different particles, thus increasing the density of modes. Nonetheless, it was still necessary to smooth the sum spectrum by Fourier Transform smoothing over 30 cm^{-1}. This does not seem to broaden the bands exceedingly. Note that, even at the low temperatures envisioned here, some anharmonicity is to be expected, which will contribute to the smoothing.

A very useful feature of the Hyperchem software is the provision for the particle to be set in motion in any of its calculated normal modes so the corresponding synchronous motions of all its atoms can be observed on the screen. To make it more quantitative, the peak (relative) displacement of each atom is represented on the screen by a vector originating in the atom. Thus small groups of atoms can be singled out, in each mode, in as much as the amplitudes of their displacements are distinctly larger than the others. In this way, a correlation can be established between such a group, a frequency and a type of vibration. This is precisely how oxygen was found to play a leading role in building up the three features of interest.

3. Numerical experiments in chemistry

Some of the experiments which led to the results stated above are listed in Table 1. Each row describes one particle by the total number of its atoms, the abundances of O, S and N and of the different environments of O: OH, O bridge and as a member of a 5-membered, otherwise carbonaceous, ring. The other, dominant atoms are, of course, C and H, in roughly equal numbers. Also given are the sums of IR intensities of the vibrational modes falling in the 3 bands of interest: I(30), I(26) and I(20), respectively, in km/mole; based on the observations of HVK, the limiting wavenumbers of these are taken to be 200-350, 350-450 and 450-525 cm^{-1}. The total intensities will help determine the band(s) for which the given type of particle is best suited in the course of fitting a particular observed spectrum (column 13). The last column lists the number of such particles entering the particular fit achieved in Sect. 4. Since the size of a dust particle is not defined here, such numbers are only meaningful in relative value.

1) The first particle (Fig. 1) is taken as a reference (R) because, in a previous study of the UIBs (Papoular 2000), it was found to display both the 30 and 20 features as well as the UIBs.

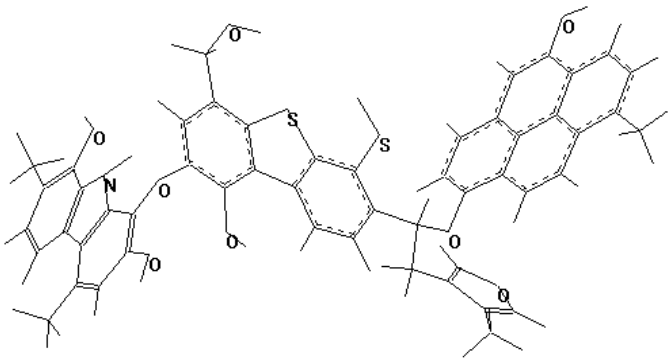

Fig. 1. The optimized reference macromolecule: R in Table 1. C and H are not labeled

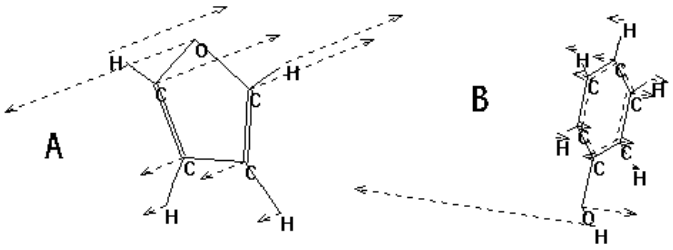

Fig. 2a and b.

It is composed of 1 pyrene (4 pericondensed (compact) benzene rings) and 2 groups of 3 catacondensed (linear) rings including pentagonal rings. These substructures are linked together by CH_2 and O bridges. Upon minimization of its potential energy, such a structure folds in upon itself, extending in 3D space. The merging and bonding of several such macromolecules will form an amorphous, mainly carbonaceous, solid. This structure was inspired by the works of chemists who developed macromolecular models of coals and soot (see review by Speight 1994) and kerogens, which are amorphous carbonaceous materials found both in the earth and in meteorites (see Behar and Vandenbroucke 1986). The other macromolecules are discussed below in logical rather chronological order.

2) The visual analysis of the motion of atoms of particle (1) in the 30-band modes revealed that the heteroatoms suffered particularly large displacements. This hint led to particle (2), in which all heteroatoms were replaced by C and H atoms. This dramatically reduced the number and intensities of modes in the whole range of interest, 200-525 cm^{-1} (19-50 μm). Remarkably, the same happened in the mid-IR UIB range (1000-1800 cm^{-1}). This strongly suggests that *one or more of the three minor atomic species must be present in the carriers of the corresponding features*. We shall leave the detailed behaviour of the UIBs outside the scope of this paper.

3) The suppression of hydroxy (OH) groups produces nearly the same effects as in (2), except on the 20-band, which is unaffected. The analysis of motions in the latter modes reveals strong and localized out-of-plane displacements in the pentagons which carry O (Fig. 2A) and N. In the present model, *these are the main carriers of the 20-band, but the OH groups dominate the other bands*. The main type of vibration of a C-O-H group in the FIR is torsion about the C-O bond, which remains still (Fig. 2B). The corresponding frequency is very sensitive to the environment: it shifts markedly upon simple displacement of the OH pair. This is why the 30-band is so broad. By contrast, the 20-band is narrow because its modes are less sensitive to the environment (more localized). Signatures of the presence of O- and N-pentagons also occur in the near IR, at about 3130 and 3400 cm^{-1}, respectively (3.2 and 2.95 μm).

4) The modes in the 26-band are mainly skeleton, out-of-plane motions, not associated with small groups of atoms but with many carbon rings simultaneously. They can only show up in the spectum if symmetry allows the IR activity, I, to differ from zero. The highly symmetric pericondensed clusters, such as pyrene or coronene therefore cannot exhibit this band; nor the other two, which are associated with non-aromatic structures (like (2) and (3)). However, linking them together by O or CH_2 bridges breaks the symmetry of the whole structure and the 26-band acquires some IR activity. It is remarkable that the two other bands remain weak. *This type of structure will therefore best help fitting the 26-band*. It is illustrated by particle (4), made up of 1 benzene, 1 anthracene (3 rings in a straight line), 2 phenantrenes (3 rings in a bent line) and a pyrene linked by O bridges.

5) The foregoing suggests that *eliminating aromatic clusters and O- and N-substituted pentagons and increasing the number of OH groups will favour the 30-band over the others*. This is illustrated by particle (5), composed of a phenantrene-like molecule linked to a pure carbon pentagon by 2 CH_2 groups, with some peripheral H's being substituted by OH and CH_3 groups.

6) Note that the addition of OH groups not only creates new modes but also enhances preexisting modes by breaking symmetries. This is illustrated by adding OH groups to structure (4) to obtain (6).

7) This is also true for O-bridges as illustrated in structure (7): basically, 3 phenantrene-like particles linked by O-bridges.

8) Sulfur does not seem to contribute notably to the three bands. However, when substituted in an aromatic ring as an SH group, it does produce strong torsional modes below 200 cm^{-1}; no relevant observation in this range is available at this time. It also contributes a strong SH stretch mode near 3900 cm^{-1} (2.56 μm), as does hydroxy.

Nitrogen contributes strongly to the 20-band when substituted in a 5-membered carbon ring (cf. (3)). An isolated signature of its presence also occurs as a NH stretch near 3390 cm^{-1} (2.95 μm). Future observations in the mid-IR may thus constrain the abundances of such groups in the dust. In the meantime, it is useful to explore structures similar to (1) but lacking the naturally rare N: (8) is one such.

9)This structure is similar to (8) but also lacks the SH group.

10) This structure is similar to (3) but also lacks the N atom, which makes it the least IR-active of all in the FIR.

Statistics over all experiments lead to the following ranges of average IR intensity per mode in bands 30, 26 and 20 respectively: 7-11,1-1.5 and 2-4 km/mole. As a consequence, and taking into account the likely relative abundances of O in the

forms of OH, O-bridge and O-pentagon, it appears that *the 30-band will be dominant and ubiquitous, while the other two will generally be much weaker and have varying intensities relative to each other*. This is borne out in HVK.

Most importantly, in this model, *all three bands must appear together (albeit with different relative intensities) and accompanied by strong and broad bands in the mid-IR range of the UIBs* as long as the heteroatoms have not been expelled from the dust by interstellar processing. According to Table 4 of HVK, this seems to be indeed the case up to the PN stage of evolution.

An interesting consequence is that the modelling of the three bands to fit observations can help predict the spectral distribution in the mid- and near-IR.

4. An example

The procedure outlined in Sect. 3 was applied to the spectra in Fig. 8 of HVK. Plotted in ordinate against wavelength, λ, is the ratio of total (feature+continuum) spectral intensity over the spectral intensity of the continuum. At a given λ, this ratio is equal to $\frac{\alpha_f}{\alpha_c}+1$, where α_f and α_c are the feature and continuum absorbances. In HVK, α_c was taken to be that of Rouleau and Martin's BE1 brand of hydrogenated amorphous carbon (1991). For this material, $\alpha_c \sim 2.7\,10^4\lambda^{-1.2}$ cm^{-1}. Now, for all materials, α=10^2 I C/Δ, where C is the molar concentration (mole/l) and Δ the spectral resolution (cm^{-1}). Hence, our fitting function is

$$Z(\lambda) = CstI_f(\lambda)\lambda^{1.2} + 1, \quad (1)$$

where I$_f$ is the smoothed sum of the mode intensities over all molecular types in Table 1, weighted by the number of each type; Cst= C/270Δ. The fitting procedure consisted in choosing an adequate combination of particles and, then, trying different values of Cst to approach the spectral shape obtained by HVK for the given object. In the present example (IRAS 22574+6609), the best combination of types is given by the numbers in the last column of Table 1 and Cst= 1/1050. The corresponding Z(λ) is shown in Fig. 3 (cf. Fig. 8 of HVK). Note the small concentrations of oxygen required.

The main defect of this qualitative fit appears to be the weakness of the blue wing of the "30" feature between 22 and 30 μm and the resulting dip near 32 μm. More work is needed to explore this range with a wider variety of structures than has been the case here. However, the discrepancy may also point to the need for a model of the absorbance by surface plasma resonance

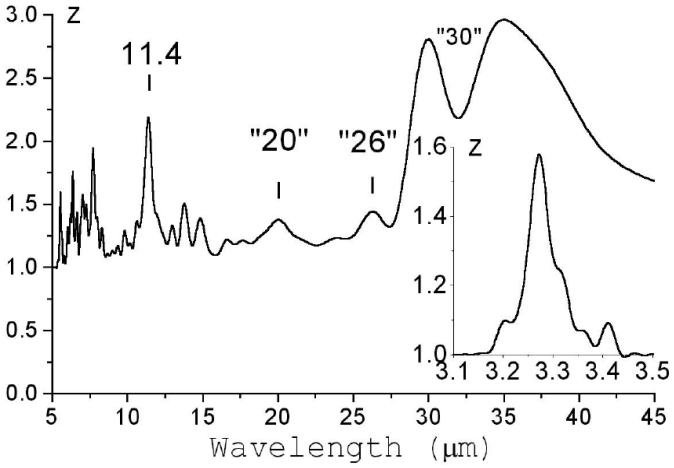

Fig. 3. IRAS 22574+6609: I(feature)/I(continuum)+1 (model). Cf. observation in HVK, Fig. 8. Insert: the stretch range enlarged.

of the "free" electrons in the aromatic components (Cody et al. 1990), which is not accounted for in the available chemical codes nor by the experimental absorbance of hydrogenated amorphous carbon (because of lack of aromaticity).

It is a pleasure to thank the referee, Dr Kevin Volk, for his comments and suggestions.

References

Behar F. and Vandenbroucke M. 1986, Rev. Inst. Fr. Petrole,41,2
Cody J. Jr at al. 1990, in Cody G, Geballe T. and Sheng P., Physical phenomena in granular materials, MRS Symp. Proc. 195, MRS, Pittsburgh
Forrest W., Houck J. and McCarthy J. 1981, ApJ 248,195
Hrivnak B., Volk K. and Kwok S. 2000, ApJ 535,275 (HVK)
Kwok S., Volk K. and Hrivnak B. 1989, ApJ 345,L51
Omont A. et al. 1995, ApJ 454,819
Papoular R. et al. 1996, A&A 315,222
Papoular R. 2000, A&A 359,397
Papoular R., Spectrochimica Acta, submitted
Rouleau F. and Martin P. 1991, ApJ 377,526
Speight J. 1994, Appl. Spectr. Rev. 29,117
Stewart J. 1989, J. Comp. Chem. 10,209
Szczerba R., Henning Th., Volk K., Kwok S. and Cox. P. 1999, A&A 345,L39
Volk K., Kwok S. and Hrivnak B. 1999, ApJ 516,L99
Volk K., Xiong G.-Z. and Kwok S. 2000, ApJ 530,408
von Helden G. et al. 2000, Science 288, 313